A climatology of low level wind regimes over Central America using a weather type classification approach

Fernán Sáenz[1]* and Ana M. Durán-Quesada[1,2]

[1] Centre for Geophysical Research, University of Costa Rica, San José, Costa Rica, [2] Department of Atmospheric, Oceanic and Planetary Physics, School of Physics, University of Costa Rica, San José, Costa Rica

Based on the potential of the weather types classification method to study synoptic features, this study proposes the application of such methodology for the identification of the main large scale patterns related with weather in Central America. Using ERA Interim low-level winds in a domain that encompasses the intra-Americas sea, the eastern tropical Pacific, southern North America, Central America and northern South America, the K-means clustering algorithm was applied to find recurrent regimes of low-level winds. Eleven regimes were identified and good coherency between the results and known features of regional circulation was found. It was determined that the main large scale patterns can be either locally forced or a response to tropical-extratropical interactions. Moreover, the local forcing dominates the summer regimes whereas mid latitude interactions lead to winter regimes. The study of the relationship between the large scale patterns and regional precipitation shows that winter regimes are related with the Caribbean-Pacific precipitation seesaw. Summer regimes, on the other hand, enhance the Caribbean-Pacific precipitation with contrasting distribution as a function of the dominant regimes. A strong influence of ENSO on the frequency and duration of the regimes was found. It was determined that the specific effect of ENSO on the regimes depends on whether the circulation is locally forced or lead by the interaction between the tropics and the mid-latitudes. The study of the cold surges using the information of the identified regimes revealed that three regimes are linkable with the occurrence of cold surges that affect Central America and its precipitation. As the winter regimes are largely dependent of mid-latitude interaction with the tropics, the effect that ENSO has on the Jet Stream is reflected in the winter regimes. An automated analysis of large scale conditions based on reanalysis and/or model data seems useful for both dynamical studies and as a tool to support forecasting. The application of the approach implemented in this study may be promising to improve current understanding on how large scale conditions affect regional weather.

Keywords: Central America, precipitation, weather type, wind, cold surge

Introduction

Central America is a narrow portion of land surrounded by the Caribbean Sea and the Eastern tropical Pacific (ETPac). Regional weather and climate are strongly influenced by warm SSTs, easterly

winds, large tropospheric moisture content and steep topography. The regional SST features warm waters phased sequentially from the Eastern North Pacific and west of Central America to the Intra Americas Sea (IAS). This distribution is known as the Western Hemisphere Warm Pool (WHWP) and traditionally, it is defined as enclosed by the 28.5 C isotherm (Wang and Enfield, 2001). The WHWP is highlighted for its potential role to force local winds, precipitation and hurricanes (Wang et al., 2007). The main feature of the regional winds is the Caribbean Low Level Jet (CLLJ). The CLLJ exhibits its primary maximum during summer (zonal wind speed up to 18 m/s) and a secondary maximum in winter (Amador, 1998, 2008; Wang et al., 2007). The CLLJ is important due to its relationship with the regional distribution of precipitation (Magaña et al., 1999), inhibition of deep convection organization and cyclones activity (Wang and Lee, 2007). The CLLJ contributes to the generation of orographic precipitation and the enhancement of the eastward divergence of the moisture flux (Amador, 2008; Muñoz et al., 2008; Cook and Vizy, 2010; Durán-Quesada et al., 2010). Regional distribution of precipitation shows a bimodal behavior. The decrease of precipitation during summer, known as the Mid Summer Drought (MSD) is related with the low level wind regime and SST distribution (Magaña et al., 1999; Small et al., 2007). The cyclone activity, both in the tropical Atlantic and the ETPac (Amador et al., 2010), as well as the less studied intrusion of cold air masses (Schultz et al., 1998; Zárate, 2013) are also part of regional weather and climate.

On the interannual scale, regional variability is lead by the effect of modes at different scales. The North Atlantic Oscillation (NAO, Rogers, 1984) is associated with SST in the Tropical North Atlantic (TNA), the size of the WHWP and the CLLJ. According to Malmgren et al. (1998), the seasonal variations of the NAO may influence the IAS easterly winds and precipitation. Warm Pacific Decadal Oscillation (PDO, Mantua et al., 1997) phases have been found associated with anomalously dry periods in the eastern coast of Central America (Méndez and Magaña, 2010). The Atlantic Multi-Decadal Oscillation (AMO, Kerr, 2000; Knight et al., 2006) signal has been found to be linked with precipitation variations in the Caribbean (Giannini et al., 2003). Gamble and Curtis (2008) suggested that the decrease in the moisture transport from the Gulf of Mexico to northwestern Mexico during positive AMO may be related with a reduction in precipitation. Wetter (drier) conditions over Central America (north-east Brazil) during JJA (DJF) were also found by Zhang and Delworth (2006) for positive AMO. The most studied variability mode in the regional context is the El Niño-Southern Oscillation (Cane et al., 1986 and references therein). Global scale studies show that ENSO is strongly linked with interannual variability of global rainfall (Dai and Wigley, 2000). Regional studies on the Caribbean relate an increase (decrease) of precipitation with cold (warm) ENSO events. Goldenberg and Shapiro (1996), Bell and Chelliah (2006) among others, reported a decrease in the intensity of Atlantic cyclones during warm ENSO events. Schultz et al. (1998) presented results supporting the hypothesis that the number of cold surges penetrating Mexico and Central America is more likely to increase during warm ENSO events.

Unlike for the tropics, the influence of the large scale processes on the high frequency variability at regional scales has been studied thoroughly for mid and high latitudes (e.g., Lamb, 1950; Trigo and DaCamara, 2000; Cortesi et al., 2013). Despite weather phenomena affecting the Intra Americas Seas, such as tropical cyclones have been widely studied, the intrusion of cold air masses into the tropics requires more research. Cold surges are observed confined to the lower troposphere to the east of the main mountain ranges, with a north-south oriented axis and duration between 2 days and 1 week (Garreaud, 2001). Cold surges in Central America and the Intra Americas Sea region have been identified by González (1999), Magaña and Vázquez (2000), Brenes et al. (2003) and more recently Zárate (2013). Reding (1992) presented a climatological study of Central American Cold Surges (CACS hereafter) using surface analysis and satellite imagery. Schultz et al. (1997) analyzed the development of a cold surge associated with a super storm in the eastern United States of America in 1993, which largely affected Central America and Mexico. Schultz et al. (1998) proposed five categories of cold surges for winters between 1978 and 1989 based on observational data from surface stations and upper air measurements. In their classification, each category is linked with a different wind regime, temperature drop and southernmost penetration.

The analysis of circulation patterns is useful to study regions like Central America, as the identification of atmospheric flow regimes performs a reasonable characterization of the large scale circulation on a predefined geographic domain. According to Molteni et al. (2006), these regimes can be regarded as points of statistical equilibrium, in which, the dynamical tendencies of the large scale flow are balanced by the non-linear interactions of the high-frequency transients. Clustering analysis can be used to identify a limited number of partitions of the phase space. Therefore, the variability of each partition is small compared to the variability of the mean state of the partitions. There are some applications of this approach for tropical regions. Moron et al. (2008) identified daily weather types in western Africa from ERA-40 wind fields and related them to precipitation over Senegal. Moron et al. (2010) associated daily weather types to monsoonal rainfall over Indonesia and Qian et al. (2010) linked those clusters to the diurnal cycle of precipitation on Java Island.

This work is motivated by the importance of day to day variability for regional weather and climate and the reduced number of studies in this subject over the region of interest in this study. The proposed work explores the reliability of the application of weather type analysis to study the main large scale patterns that characterize regional circulation over the region of interest in this study. The identification of main synoptic patterns, the evolution of large scale conditions and the relationship between the synoptic patterns and regional precipitation are the focus of this study. This research presents the application of a simple automated classification method to study the large scale circulation that affects the Central American region, the existence of recurrent low-level wind patterns and their effect on regional weather. A special focus is given to the intrusion of cold air masses. As the effect of ENSO is of particular importance, this work also aims to explore the response of the identified patterns to ENSO,

in terms of both intensity and frequency. The study is organized as follows, an introduction with background information on regional weather, climate and their variability that may be useful for reference was given in Section Introduction; Section Data and Methods describes the data and method used. The results are provided in 4 sub sections; the description of the weather types identified and the relationship between the patterns and precipitation are provided in Section Description of the Main Circulation Patterns and Relationship between the Identified Regimes and Precipitation in Central America respectively, the analysis of the response of the weather patterns to ENSO is given in Section Response of the Circulation Regimes to ENSO and Section Inferring the Intrusion of Cold Surges to Central America from Large Scale Patterns contains a detailed analysis of the case of the cold surges. The discussion is provided in Section Discussion and Section Conclusions presents a summary of the analysis, conclusions and further proposed research work.

Data and Methods

Data

Reanalysis Data

The signature of regional climatic features such as the CLLJ (Amador, 2008), MSD (Karnauskas et al., 2013) and cold surges (Garreaud, 2001) is strong at the low-levels. Wind fields at 925 and 850 hPa were extracted from de ERA-Interim reanalysis (Dee et al., 2011) as descriptors of the low-level atmospheric circulation. Complementary, geopotential height at 500 hPa was also retrieved from the ERA-Interim dataset. The daily data spans from 1979 to 2012 and encompasses an area from 8 N to 25 N and from 260 E to 295 E (see the white box in **Figure 1**).

Low-level wind data were normalized subtracting the time series mean to each grid point and dividing it by its standard deviation. In search of computational efficiency, Principal

FIGURE 1 | Region of interest. Geographic domain for the ERA-interim data used in the clustering algorithm is enclosed by the white box.

Components Analysis (PCA) was applied to the data. The 62 first components accounted for 95% of the variance; this implied a significant reduction in data dimensionality, computing time and resources. As the objective of the work is to describe large scale features, the decomposition procedure serves to filter noise that could affect the cluster analysis. To analyze the atmospheric configuration related to mean state of each cluster, composites of wind fields and geopotential height at 925 hPa were computed. Seasonal frequency charts were also drawn in order to analyze if there was a seasonal preference in regime occurrence (not shown).

Precipitation Data

Tropical Rainfall Measuring Mission (TRMM, Simpson et al., 1988) Multi-Satellite Precipitation Analysis (TMPA, Huffman et al., 2010) was used as an approximate of daily precipitation. We are aware that this data is not homogeneous and its quality depends on the availability of source data of high quality rain gage data for the rescaling. However, due to the lack of good quality and long term precipitation observation networks in the region and the known biases for this variable in the reanalyses, the 3B42 version 7 dataset, in a $0.25° \times 0.25°$ grid with 3-h temporal resolution for the 1998–2012 period was consider fair enough to be used to compute daily aggregates.

Method

Cluster analysis has been widely used for circulation patterns recognition (ej. Cheng and Wallace, 1993; Straus and Molteni, 2004; Casola and Wallace, 2007). This method divides a set of N-dimensional data vectors by grouping them into categories. The distance of the vector to the center of each group in an N-dimensional space is the criterion used to assign a vector to a category. Distance can be measured in multiple ways, being the Euclidean distance the simplest. The k-means clustering method (see MacQueen, 1967 for more details) is herein implemented. One of the major draw backs of the k-means algorithm is that the number of categories or clusters, k, must be specified a priori. To find a suitable number of clusters reducing the subjectivity, a combination of methods proposed by Michelangeli et al. (1995) and Cheng and Wallace (1993) was applied. This procedure has been previously used by Moron et al. (2008) and follows the general five-step procedure described by Molteni et al. (2006). The method employed by Michelangeli et al. (1995) relays on the fact that k-means results could be dependent on initial seeds and uses the similarity between the results of different clustering repetitions (partitions) to assess this dependency. To measure the similarity between partitions, Cheng and Wallace (1993) proposed a method based on centroid correlations. Following Cheng and Wallace (1993):

(a) Given two partitions P1 and P2, of k clusters, correlations between centroids are placed in a matrix

(b) For the ith row the maximum is computed and saved as B(i), this value is the correlation between the ith cluster in P1 and its analog in P2

(c) The minimum value in vector B is taken as the pattern correlation between P1 and P2 and denoted c(P1,P2). To generalize this procedure to M partitions in the same k number of
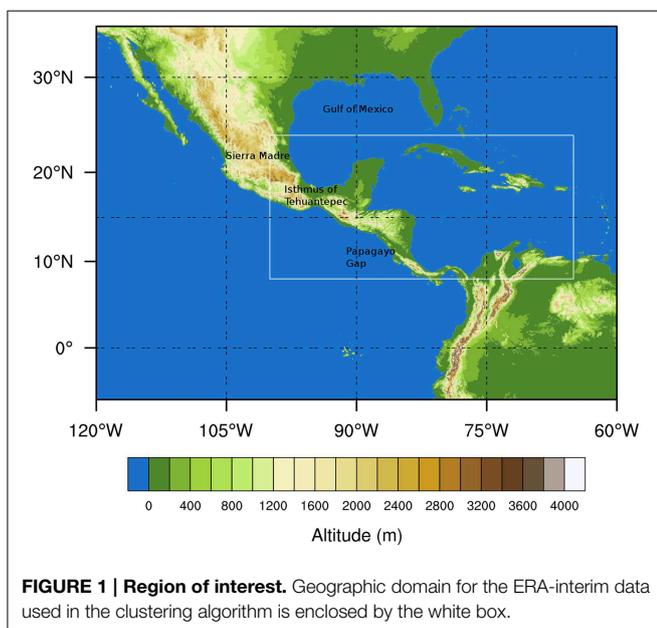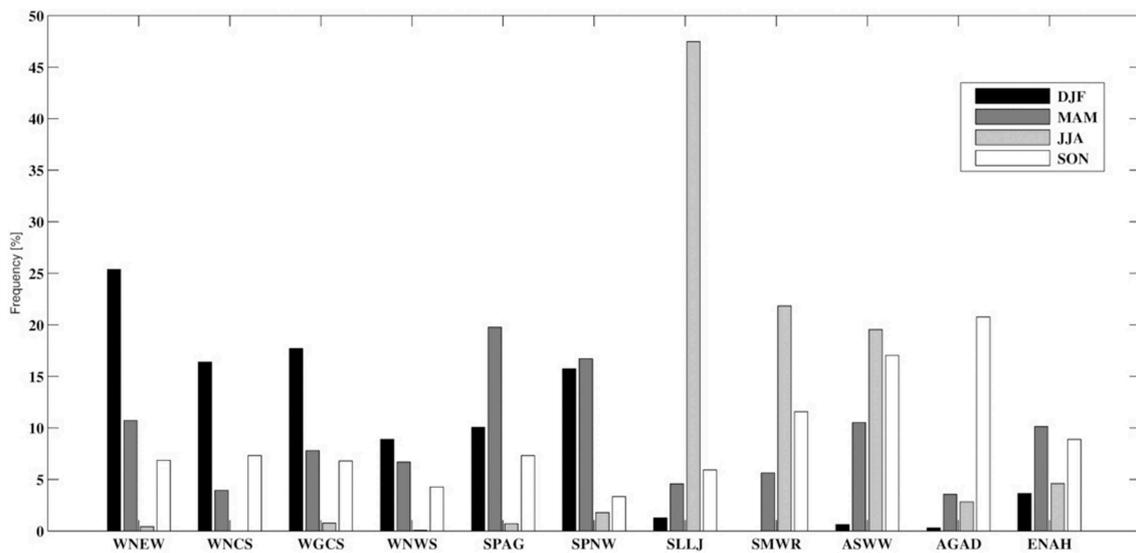
FIGURE 2 | Relative seasonal frequencies showing the dominance of the 11 regimes found. For each season all regime frequencies should sum up to a 100%.

clusters, Michelangeli et al. (1995) defined the classifiability index CI(k):

$$CI\left(k\right) = \frac{1}{M(M-1)} \sum_{1:m \neq m'}^{M} C(Pa_m\left(k\right), Pa_{m'}\left(k\right))$$

The classifiability index varies between 0 and 1. A value of 1 means that M partitions with fixed k produce exactly the same k clusters. For different values of k, the more reliable as predefined number of clusters, is the one that produces the highest CI while maintaining statistical significance.

In this work, the number M of different partitions was set to 100 and CI (k) was computed for $k = 2,..,15$. To assess statistical significance, CI (k) was computed 100 times for every k using quasi-random red-noise data drawn from the original data set. The highest, statistically significant at 99% according to the red-noise test, CI value from the observed data set was found $k = 5$, same as the number of clusters used by Schultz et al. (1998). However, a classification in such small number of clusters would result in very general circulation patterns, mainly considering that a number of 5 patterns of CACS were found by Schultz et al. (1998) while classifying only winter circulation. Therefore, the value $k = 11$, which ensured a high significance (83.5% in this case), was used instead; using an a priori number of 11 clusters assures high statistical significance and is not as small so that only broad general circulations patterns can be identified.

Results

Description of the Main Circulation Patterns

Two large categories can be used to group the 11 circulation patterns found as pure seasonal or transitional patterns. No pure seasonal patterns were found for spring, suggesting that those months are dominated by transition signals. The names are based on the dynamical features of the regimes, **Figure 2** shows the frequency of each regime, from which the seasonality of the regimes can be noticed. **Figure 1** shows some of the more relevant topographic features of the study area for reader's reference.

Winter North Eastern Winds (WNEW)

This is the most frequent regime during winter; it is likely to occur, on average, up to 10 days per month during winter time. The persistence of this pattern is typically 3 days. The circulation linked to this pattern is featured by northeasterly winds over the Caribbean, which is related to a geopotential maximum off the East coast of the United States of America (USA). These winds cross the Central American Isthmus and reach the ETPac (**Figure 3A**). The large scale features of this regime are typically observed during the winter maximum of the CLLJ. The trans-isthmic flow is enhanced mainly through the Papagayo gap. The 500 hPa geopotential height, depicted in **Figure 4A**, shows a mid-tropospheric trough over the North Atlantic and USA region, in contrast with relatively quiescent weather conditions over the Gulf of Mexico.

Winter Northern Cold Surge (WNCS)

Each episode of the WNCS regime tends to last between 1 and 2 days (maximum duration, up to 3 days is found in November). This regime is characterized by an eastward displacement of the North Atlantic Subtropical High (NASH) and a geopotential maximum centered at the southeast USA coast. This maximum extends into the sea and is bounded to the West by the Sierra Madre mountain range (**Figure 3B**). The mean low-level wind field features an anti cyclonic gyre in which the winds converge with the weakened trade winds; this enhances winds over the Central American Isthmus from North to the northeast. The intensified flow crosses the continent through the topographic
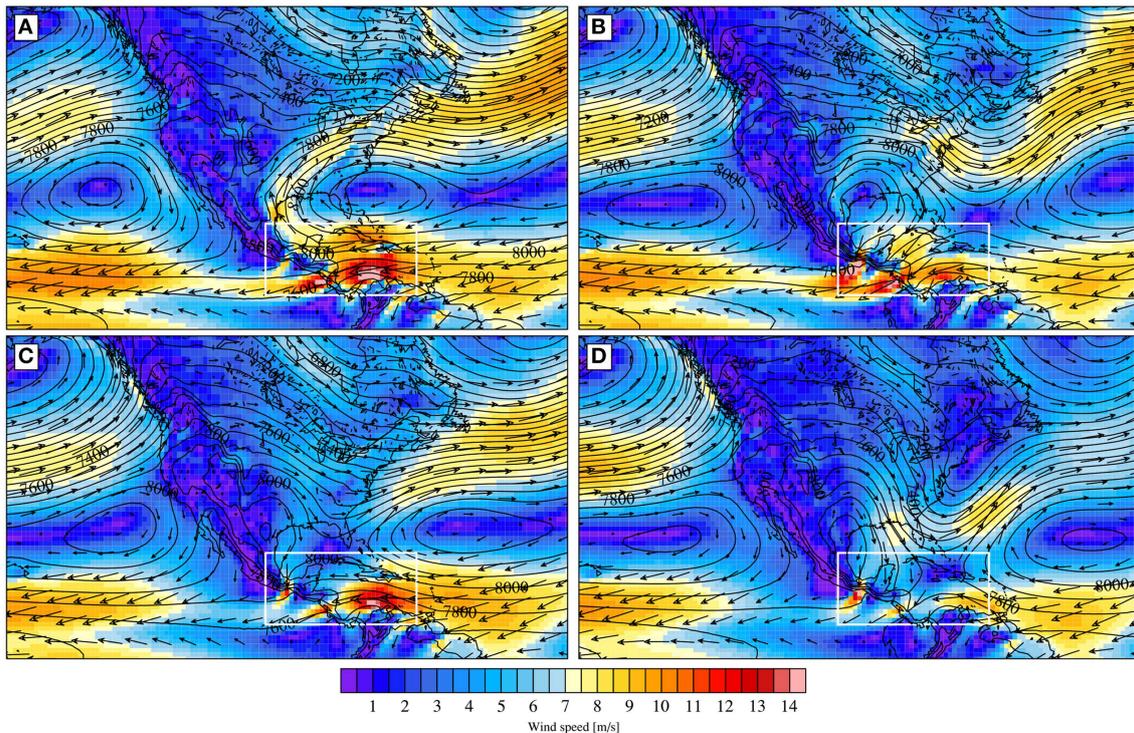
FIGURE 3 | Composited large-scale patterns at 925 hPa associated with (A) WNEW, (B) WNCS, (C) WGCS, and (D) WNWS regimes. Geopotential height [m²/s²] (black contours), wind speed [m/s] (colored pixels) and wind vectors. Geographic domain for the ERA-interim data used in the clustering algorithm is enclosed by the white box.

passes, producing gap winds over the Papagayo and Tehuantepec regions (**Figure 3B**). The mean horizontal low-level fields of this regime are coherent with the low level structure of a typical cold surge entering the Gulf region from central Canada (Henry, 1979; Schultz et al., 1998). In this regime, the trough penetrates into the Gulf of Mexico and the anticyclonic gyre in the Gulf of Mexico is more defined. The easterly flow is even more confined than for WNEW, enhancing trans-isthmic transport through the Gulf of Tehuantepec, in good agreement with observations as reported by Chelton et al. (2000). **Figure 4B** shows cyclonic anomalies at 500 hPa over Central America and the adjacent Pacific Ocean.

Winter Gulf Cold Surge (WGCS)

Observed during winter, this regime appears nearly 17% of the days (**Figure 2**), with a duration between 1 and 2 days. Two geopotential height maxima are observed for this regime, one east of the Sierra Madre and the other related to a westward displacement of the NASH (**Figure 3C**). The low-level wind field is lead by anticyclonic winds related to the NASH, northerly winds over the Gulf region and gap winds off the Central America's Pacific coast (**Figure 3C**). In this regime, the trans-isthmic flow is reduced compared to previous regimes. As the anticyclonic gyre in the Gulf of Mexico is not fully developed, the wind field is not strongly constrained. A mid tropospheric trough enters the east coast of North America, with the divergence

field stretching along the storm track (**Figure 4C**). This regime is only related to cold surges that do not reach the Central American region; this because the NASH constrains the southward displacement of the cold air that is channeled by the topography.

Winter North Western Surge (WNWS)

WNWS is more frequent during spring and winter (**Figure 2**), its mean duration ranges between 1 and 2 days and is also important in November. Even though the distribution of geopotential is similar to the WGCS regime, WNWS differs in the following aspects: (a) the western limit of the NASH is located to the east of the Hispaniola island, allowing the formation of a trough off the USA east coast and (b) a southward displacement of the geopotential maximum is located east of the Sierra Madre mountain range. The main features of the low-level wind are weakened trades, enhanced gap winds at the Yucatan peninsula and northerlies that reach as far south as Costa Rican Caribbean coast (**Figure 3D**). Low level wind over the Central Caribbean is minimum as the Central Caribbean is featured by divergent wind flow. In the mid troposphere, the westerly flow is dominant (**Figure 4D**). These conditions provide an environment that allows the entrance of Pacific cold surges. The large scale features of this regime resemble the structure of cold surges moving from the east Pacific and reaching Central America (Henry, 1979; Schultz et al., 1998).

FIGURE 4 | Composited large-scale anomalies at 500 hPa associated with (A) WNEW, (B) WNCS, (C) WGCS, and (D) WNWS regimes. Geopotential anomalies (colored pixels) and anomalous wind field (vectors).
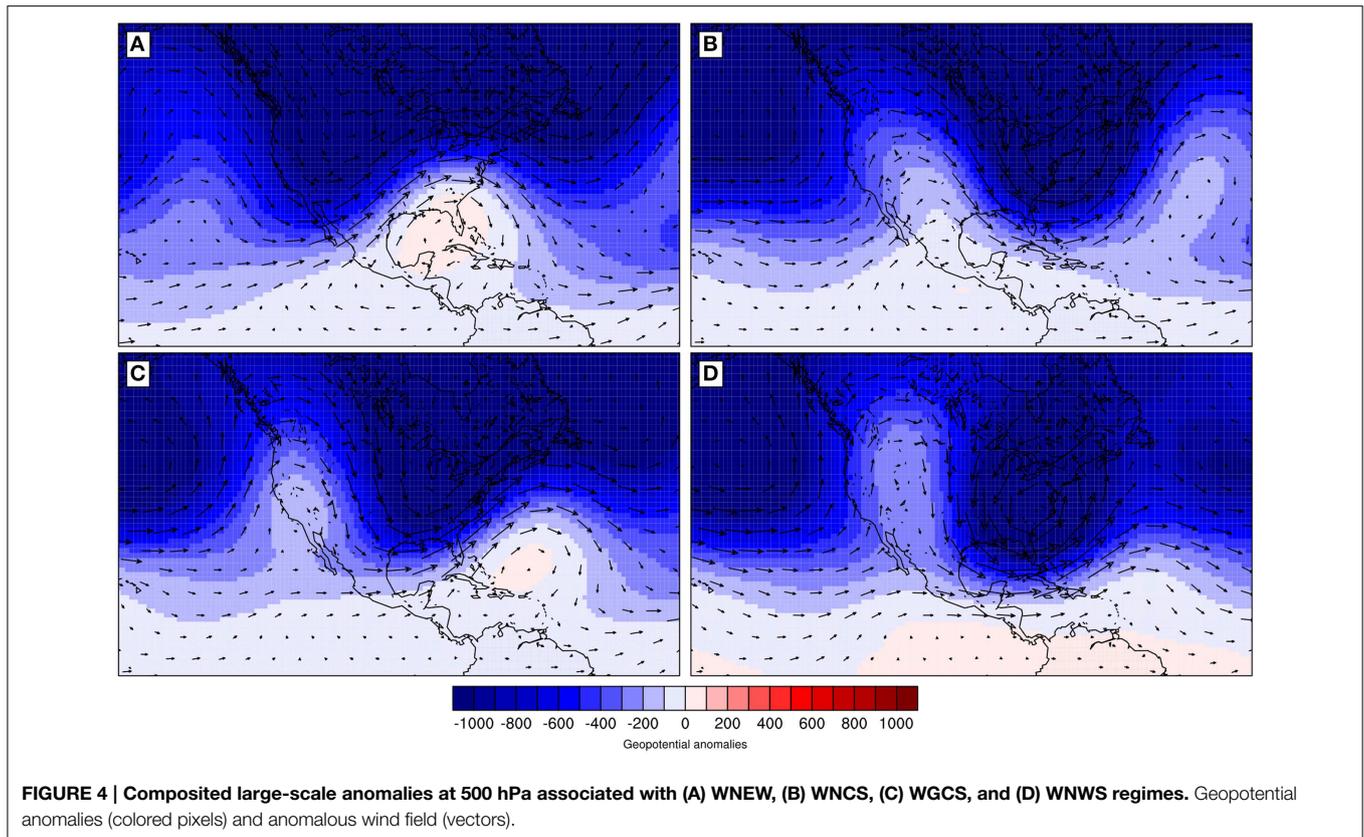
Spring Anti Cyclonic Winds at the Gulf (SPAG)

This regime is more frequent during March and April (even when observed during winter and autumn). The largest persistence in the number of days is 3 (during April). The mean geopotential field of this regime shows a marked eastward displacement of the NASH (**Figure 5A**). Such displacement allows the establishment of a geopotential maximum centered over Florida. The latter induces an anticyclonic gyre with low-level easterlies over the northern portion of the Caribbean Sea. The anticyclonic gyre reinforces the weakened trades, forming a shear line off the coast of Honduras and Nicaragua. For this regime, isolated mid-tropospheric troughs over the Rocky Mountains and the Atlantic off the east coast of USA are well defined (**Figure 5A**). A mid-tropospheric anomalous ridge over the Gulf of Mexico inside a wave train is clear in **Figure 6A**.

Spring NASH West (SPNW)

Almost equally frequent during spring and winter (**Figure 2**), the SPNW regime dominates the seasonal transition and it is the most frequent regime during February and March. Maximum of persistence is found to have an average duration of 2–3 days. A more developed NASH that penetrates into the Gulf of Mexico induces a low-level wind circulation with south easterlies in the Gulf region and enhanced trades over the Caribbean with intensified activity of the CLLJ (**Figure 5B**). A large mid-tropospheric ridge over the western North Atlantic and North America is the main feature of the 500 hPa geopotential height anomalies field

(**Figure 6B**). The large anomalies observed suggest a favorable environment for storm development.

Summer Low Level Jet (SLLJ)

SSLJ is the dominant summer regime (**Figure 2**). It exhibits the largest frequency (up to 47%) of the observed patterns during the summer months (observed up to 22 days in July). This regime has the largest persistence of the identified regimes as an event can last up to 10 consecutive days. Low level flow for this regime shows a reinforcement and increase in the zonal extension of the NASH. Low level winds linked to the geopotential field of this pattern feature enhanced trades over the Caribbean Sea. A low-level jet like structure is observed off the northern coast of South America and enhanced southerlies entering the Great Plains region from the Gulf coast (**Figure 5C**). The structure shown by the low level winds of this regime is consistent with the primary maximum of intensity of the CLLJ. Mid troposphere geopotential height anomalies suggest quiescent conditions for this regime (**Figure 6C**).

Summer Monsoonal Winds Regime (SMWR)

This summer regime, more frequent in early and late summer, can be also observed during autumn and less frequently in spring (**Figure 2**). The geopotential distribution features a NASH similar as for the SLLJ regime, but with a smaller maximum shifted to the East. This configuration may produce a northward veering of the trades over the Caribbean. Such veering, added to the effect
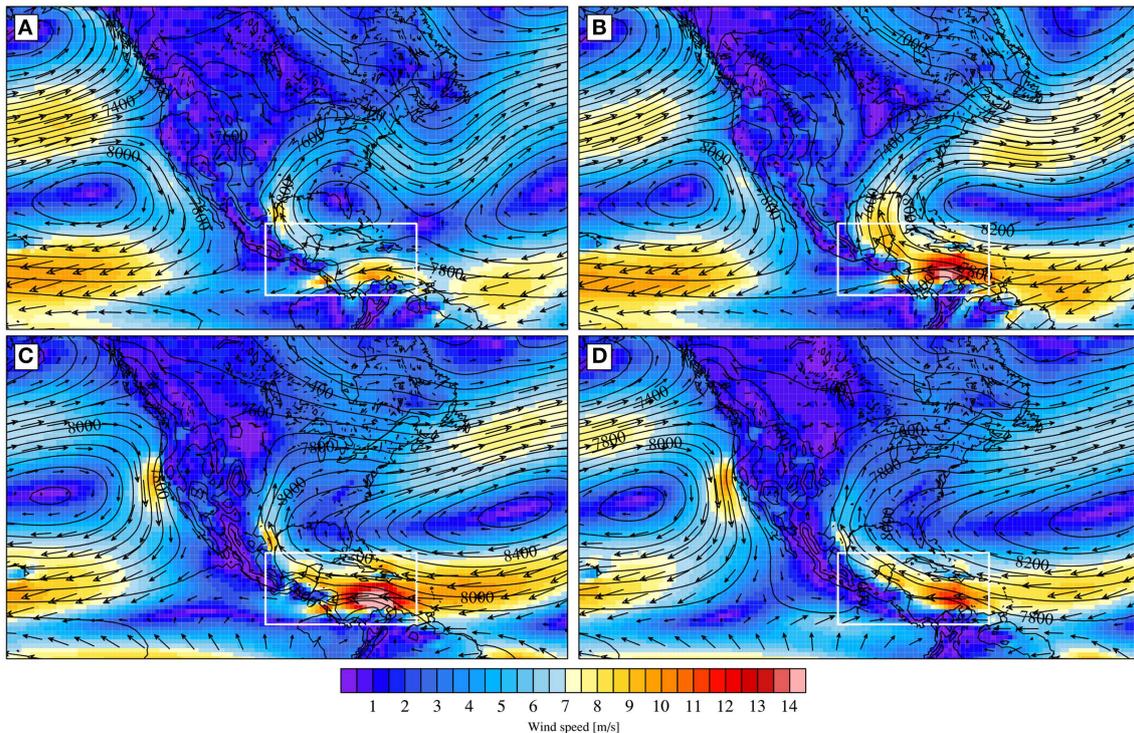
FIGURE 5 | Composited large-scale patterns at 925 hPa associated with (A) SPAG, (B) SPNW, (C) SLLJ, and (D) SMWR regimes. Geopotential height [m²/s²] (black contours), wind speed [m/s] (colored pixels) and wind vectors. Geographic domain for the ERA-interim data used in the clustering algorithm is enclosed by the white box.

of thermal forcing by the Central American isthmus, the WHWP and the enhancement of the southerly trades may induce low-level southwesterly winds that reach the Central American Pacific coast (**Figure 5D**). A mid tropospheric ridge over the west coast of North America along with the development of a cyclonic circulation west off Central American coast is observed for this regime (**Figure 6D**).

Autumn South Westerly Winds (ASWW)

ASWW is frequent during late spring, summer and early autumn (**Figure 2**). Its occurrence peaks in August and September and events last between 1 and 4 days. The mean geopotential field is characterized by a NASH displaced to the East and a secondary geopotential maximum centered over the Gulf coast of the United States. The confluence of the Trades and the easterlies related to the anticylonic gyre induced by the secondary geopotential maximum (**Figure 7A**) enhances trade winds over the Caribbean. The mid troposphere geopotential height anomalies suggest steady weather conditions (**Figure 8A**).

Autumn Geopotential Dipole Anomalies (AGAD)

AGAD is the most frequent regime during autumn and it is rarely seen in any other season (**Figure 2**). Geopotential mean field shows a weakened NASH displaced to the East. This configuration produces a geopotential anomalies field dipole. Negative anomalies are observed over the Gulf, the Caribbean and the

western tropical Atlantic (**Figure 6B**), whereas, positive anomalies are centered over the Canadian eastern coast (not shown). Reduced trade winds, that barely reach the Caribbean coast of Central America, may allow the continental thermal forcing to induce westerly winds that reach its Pacific coast (**Figure 7B**). From **Figure 8B**, it can be observed that the 500 hPa geopotential height anomalies suggest relatively positive anomalies in the eastern portion of North America. The latter is in contrast with negative values that may suggest storm activity in the Caribbean.

East North Atlantic High (ENAH)

This regime is almost equally important during spring, summer and autumn (**Figure 2**). This pattern does not persist longer than 4 days. The mean geopotential distribution of this regime shows and eastward displaced NASH. The effect on the wind patterns over the Pacific is similar to those of the SMWR regime, but with a well-defined anticyclonic structure over the tropical Atlantic-Caribbean sector (**Figure 7C**). This regime presents a unique mid tropospheric structure in which negative anomalies amplify strongly north of the Gulf of Mexico, TNA and with smaller magnitudes over the north-east Pacific (**Figure 8C**). These negative anomalies contrast with the positive anomalies all over North America. The conditions from the mid tropospheric geopotential height may suggest suitable conditions for storm development.

**FIGURE 6 | Composited large-scale anomalies at 500 hPa associated with (A) SPAG, (B) SPNW, (C) SLLJ, and (D) SMWR regimes.** Geopotential anomalies (colored pixels) and anomalous wind field (vectors).
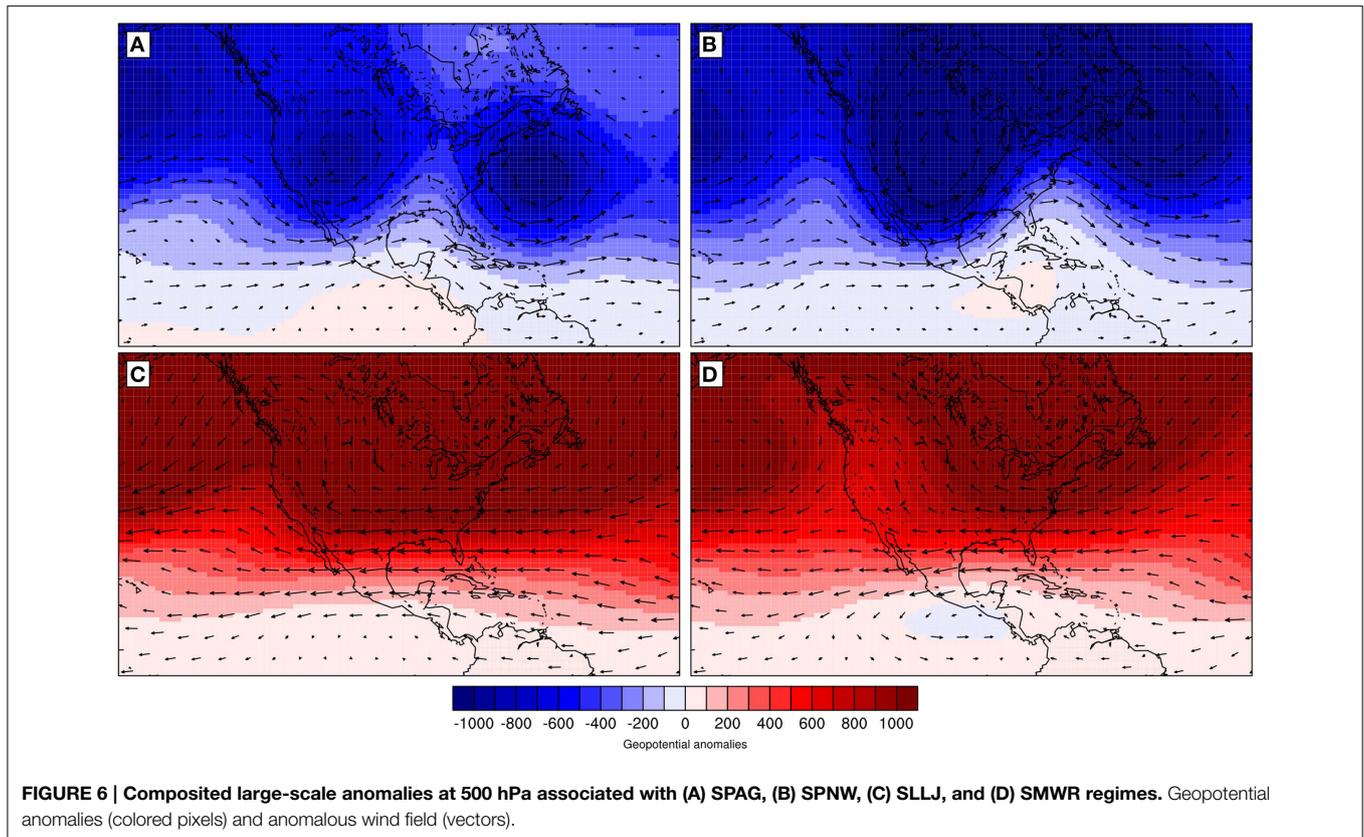
Relationship between the Identified Regimes and Precipitation in Central America

Precipitation associated with each regime is fairly consistent with the known seasonal precipitation distribution. Marked differences in precipitation fields associated with regimes that are characteristic of the same season were found. Winter months are commonly dry in most of Central America, except for some areas in the Caribbean side (Alfaro, 2000). **Figure 9** shows that, for the winter regimes, less precipitation is observed over the Pacific side of the isthmus. In contrast, more intense precipitation is observed on the Caribbean slope due to topography-forced ascend. Under WNEW conditions (**Figure 9A**), Caribbean precipitation is maximum to the east of Costa Rica and Panama. A similar pattern is observed during WNCS events, but it differs from WNEW because a secondary precipitation maximum in the east coast of Honduras is observed under the WNCS regime. When cold surges reach the Central American region (WNCS and WNWS) rainfall increases over the Caribbean shores of Honduras and Costa Rica. When cold surges reach the Gulf of Mexico, but do not move further south (WGCS), Central America is drier. Despite winter precipitation in the Caribbean slope is mainly forced by topographic effects, wind shear is important over the Isthmus when surges reach the region as will be later discussed.

Spring months are dry in Central America, consistently with the reduction in precipitation for the SPAG (**Figure 9E**) and SPNW (**Figure 9F**) regimes. Nevertheless, regimes that can be also found in spring such as WNEW (**Figure 9A**)

and WNWS (**Figure 9C**) are linked with wetter conditions in the Caribbean slope and southernmost Central America. The ASWW (**Figure 9I**) and ENAH (8.k) regimes are also related to more intense precipitation in the Pacific side. The ENAH regime, with its anomalous westerly flow, could be associated with the beginning of the rainy season in the Central American Pacific slope (Alfaro, 2000; Cortez, 2000); a reduction of atmospheric stability due to an increase in coastal ETPac SST (via latent heating) characterizes the rainy season onset for this region.

The mean conditions for the SLLJ, SMWR, and ASWW regimes are consistent with the large scale conditions that provide the environment for precipitation intensification in the region (**Figure 9I**). Those conditions are northward veering of the trades, enlargement of the WHWP with its consequent reduction of stability due to the exponential relation between SST and large low level moisture content. The dynamic fields for the SLLJ regime show the enhancement of the easterly flow along with a deeper NASH, a clear fingerprint of the CLLJ. When this regime is present, a reduction in precipitation is seen all over the Pacific side of the Isthmus. In contrast, over the Caribbean side of Costa Rica and Nicaragua, Belize and Tehuantepec, precipitation is increased (**Figure 9G**). When the SMWR regime dominates, a cyclonic wind anomaly is present at 500 hPa over Central America and its adjacent Pacific Ocean. This anomaly, which acts in conjunction with low-level convergence to enhance vertical moisture transport, is consistent with the intensification of precipitation observed in that region (**Figure 9H**).
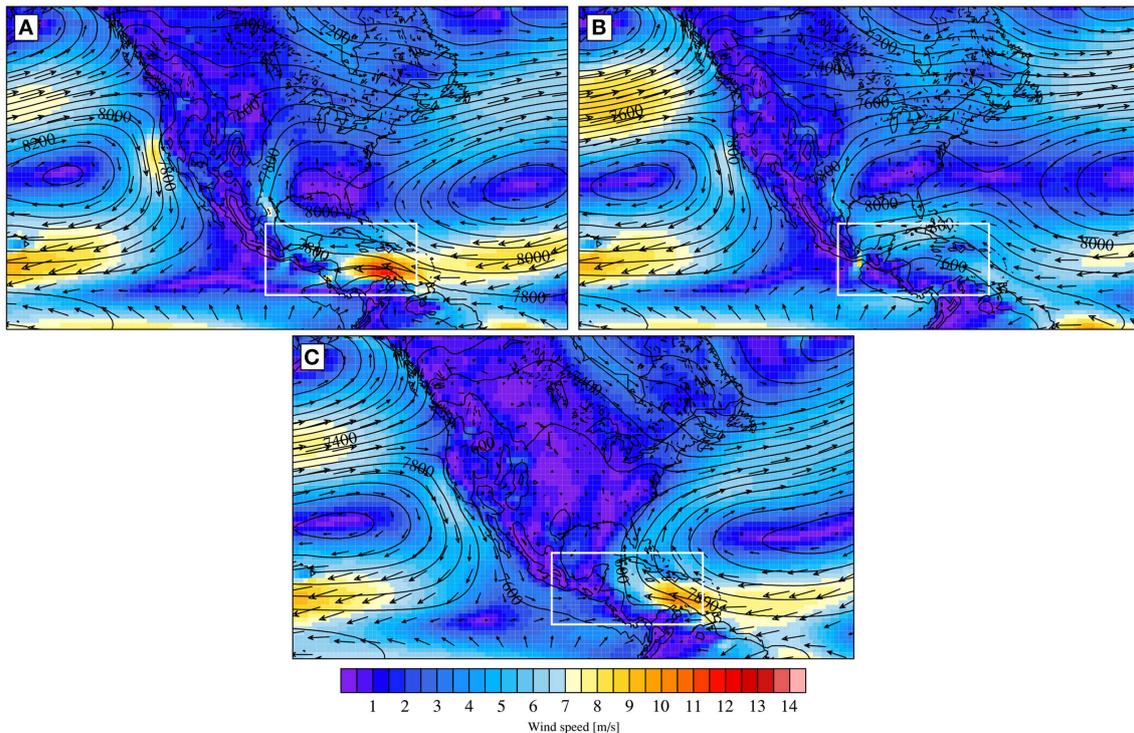
FIGURE 7 | Composited large-scale patterns at 925 hPa associated with (A) ASWW, (B) AGAD, and (C) ENAH regimes. Geopotential height [m²/s²] (black contours), wind speed [m/s] (colored pixels) and wind vectors. Geographic domain for the ERA-interim data used in the clustering algorithm is enclosed by the white box.

The autumn months are the rainiest in Central America (Alfaro, 2000). During this season, the weakening of the NASH, the establishment of the WHWP (in the Central America Pacific coastal areas and the Caribbean) and a maximum tropical cyclone activity over the Caribbean (Wang and Lee, 2007) act together to enhance rainfall in the Pacific slope. **Figure 9** shows that, for the pure autumnal regime AGAD (**Figure 9J**) as well as other regimes frequent during this season, Pacific precipitation is larger. The AGAD regime features a cyclonic anomaly at 500 hPa over the Central America and both adjacent water bodies. The mid tropospheric signal reflects a conductive environment for an intensification of precipitation over the Caribbean Sea and the Pacific coast of Central America as there is a thick layer of moisture convergence (**Figure 9J**). When ASWW is present, precipitation in Nicaragua shows a different pattern, with more (less) rain over the Caribbean (Pacific) side. The latter may be related with the presence of disturbances over the southern Caribbean such as easterly waves or tropical depressions.

Response of the Circulation Regimes to ENSO

ENSO is regarded as the strongest climate variability mode for the tropics (Pezzi and Cavalcanti, 2001; Turner et al., 2005). It is regionally known to modulate variations in precipitation (Ropelewski and Halpert, 1987). Therefore, understanding how ENSO may affect the large scale regimes found is of particular importance. Using the frequency information for the regimes and

the Multivariate ENSO Index (MEI, Wolter and Timlin, 2011) as a measure of ENSO intensity, the monthly frequency for each regime was composited for warm and cold ENSO as well as for neutral conditions according to the moderate or stronger MEI ENSO events classification. The likelihood of a regime to occur is reported as a probability ranging from 0 to 1, where 1 is equivalent to the 100% of probability to observe a determined regime.

Results shown in **Figure 10**, suggest that cold ENSO increases the probability of the WNEW (**Figure 10A**) and WNCS (**Figure 10B**). In contrast, warm ENSO phase increases the probabilities of occurrence for WGCS (**Figure 10C**) and WNWS (**Figure 10D**). The increase in the frequency of the WNWS regime (**Figure 10D**) under El Niño conditions is a response to the intensification of the wind flow through the Gulf of Mexico, suggesting the intensification of cold air intrusions. The latter is in agreement with findings by Schultz et al. (1998) that report an anomalously larger number of strong cold surges into Central America for El Niño events. Composites for precipitation (**Figure 11**) show negative anomalies up to 12 mm/day, linked with the occurrence of WNWS during warm ENSO. The increase in the number of CACS under warm ENSO leaves a drier than normal Caribbean. Pérez et al. (2014) suggest that, an increase in CACS frequency accompanied by a shortening of wavelength and lifespan, typical of positive ENSO conditions, could lead to a reduction in the precipitation caused by CACS.

FIGURE 8 | Composited large-scale anomalies at 500 hPa associated with (A) ASWW, (B) AGAD, and (C) ENAH regimes. Geopotential anomalies (colored pixels) and anomalous wind field (vectors).
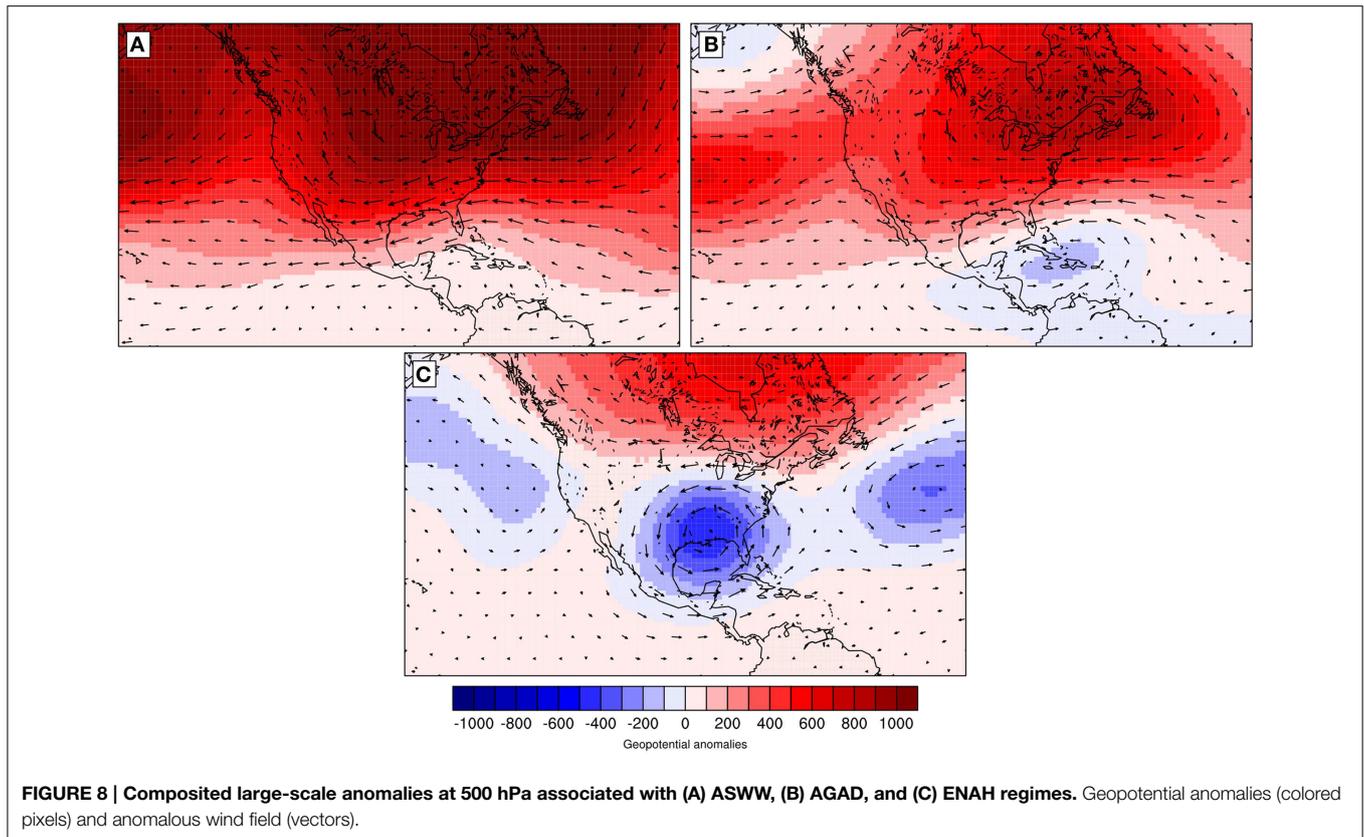
The occurrence of SPAG regime is increased as warm ENSO is linked with the intensification of the easterly flow. Despite the increase in the probability for SPAG, non-significant changes in precipitation for this regime, associated with the effect of ENSO, were found. The largest variations (up to 30%) are observed for the SLLJ during El Niño events (**Figure 10G**). The results shown are in good agreement with the fact that El Niño is linked with a stronger CLLJ (Wang, 2007; Amador, 2008). As this phase favors the intensification and expansion of the WHWP (Wang and Enfield, 2003) as well as the strengthening of the NASH, the large scale features of SLLJ are also intensified. The intensification of the CLLJ is known to be related with drier (wetter) conditions over the Caribbean (Pacific). The increase of days with a dominant SLLJ regime may be expected to be related with drier conditions. Composites for precipitation under the positive and negative phases of ENSO (**Figure 11**) show the drying of Central America (mostly over the Caribbean slope) for warm ENSO. In contrast, west off Central America, precipitation is intensified under the same ENSO phase, as shown in the anomalies (**Figure 11**). This result has a direct implication on the assessment of drier than normal summer periods and hence, a deeper MSD under El Niño. An enhanced CLLJ produces descending motion over the Pacific side which inhibits deep convection.

The response of the SMWR regime to ENSO is the most extreme of all the regimes. During July and August, the probabilities of the mode to occur increase by 40% from El Niño to La Niña conditions. For the SMWR regime (**Figure 10H**), La Niña has been associated with the intensification of the occurrence of this regime. This implies that, cold ENSO phase provides conditions that allow the enhancement of the northward veering of the Trades. An increased northward flow is known to occur under cold ENSO conditions (Yu and Wallace, 2000). The latter, in agreement with the findings that suggest a larger frequency of the pattern linked to the summer monsoonal flow during La Niña events. This result may suggest that, precipitation increases during La Niña, favored by the intensification of the monsoonal flow, mainly in northern Central America. The difference between precipitation for El Niño and La Niña, results in negative anomalies with maximum values in northern Central America. Therefore, rainfall is likely to be more intense for La Niña events during summer in dominance of the SMWR regime. This shows coherence with the expected conditions of rainfall when the monsoonal flow is enhanced, as reported by Yu and Wallace (2000).

The results found are indicative of the response of the large scale circulation linked to regional phenomena to the ENSO variability mode. Such results are relevant as they provide an important input for weather analysis and may be useful for seasonal precipitation forecasting ahead of the development of a particular ENSO phase. Note that an analysis on how the precipitation responds to the variability of the patterns due to ENSO is not presented in full detail; TRMM precipitation record is rather short for a detailed study of the interannual variability. However, a further study on this issue will be raised in a future study using a

FIGURE 9 | Composited TRMM 3B42 precipitation fields [mm/day] for (A) WNEW, (B) WNCS, (C) WGCS, (D) WNWS, (E) SPAG, (F) SPNW, (G) SLLJ, (H) SMWR, (I) ASWW, (J) AGAD, and (K) ENAH regimes.
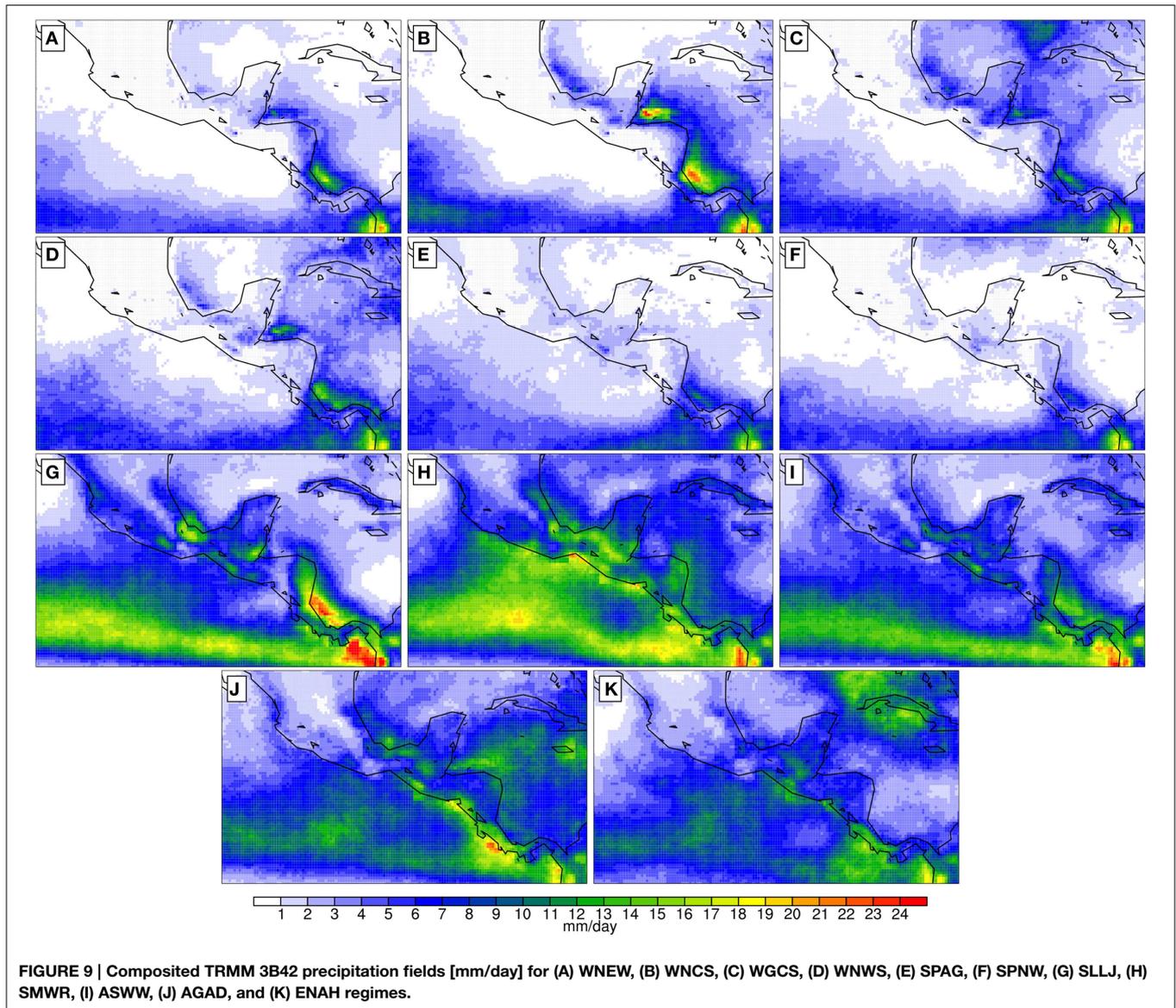
longer time span when a new high resolution blended daily precipitation dataset becomes available at the required time scales for such task.

Inferring the Intrusion of Cold Surges to Central America from Large Scale Patterns

The intrusion of cold extratropical air into the tropical regions is a phenomenon constrained to the eastern slope of major mountain ranges (Garreaud, 2001). The low-level dynamic fingerprint of cold surges located east of the Sierra Madre is used here to identify them. Previous CACS climatologies were developed using stations data, satellite imagery and rawinsonde data (Reding, 1992; Schultz et al., 1998). Those studies are suitable to test the ability of the k-means classification method to detect CACS. Reding (1992) includes a table with the onset date and duration for each of his classified CACS for the October to March season

for the period of 1979–1990. This information was used to construct a time series of days where CACS were present and used as a test bed for a time series of CACS days from the k-means method applied in this work. For this comparison, CACS days are defined as days when WNCS and WNWS regimes are present; WGCS regime days were not taken into account because when this regime is present CACS reach as south as the Gulf of Mexico, this creates inconsistencies with Reading definition of CACS. The automated classification based on large scale patterns, herein used, is able to capture up to 78% of the overlapping days in which Reding (1992) detected cold surges. Differences in the nature of the data as well as the spatial and temporal resolution could justify the difference between the numbers of days with CACS identified for the two methods.

As mentioned before, the three regimes related to cold CACS reproduce the structure of surges of different origins, based on

FIGURE 10 | Monthly probabilities of occurrence under each ENSO phase for every regime. Ordinate axis scales are not the same for every subplot.
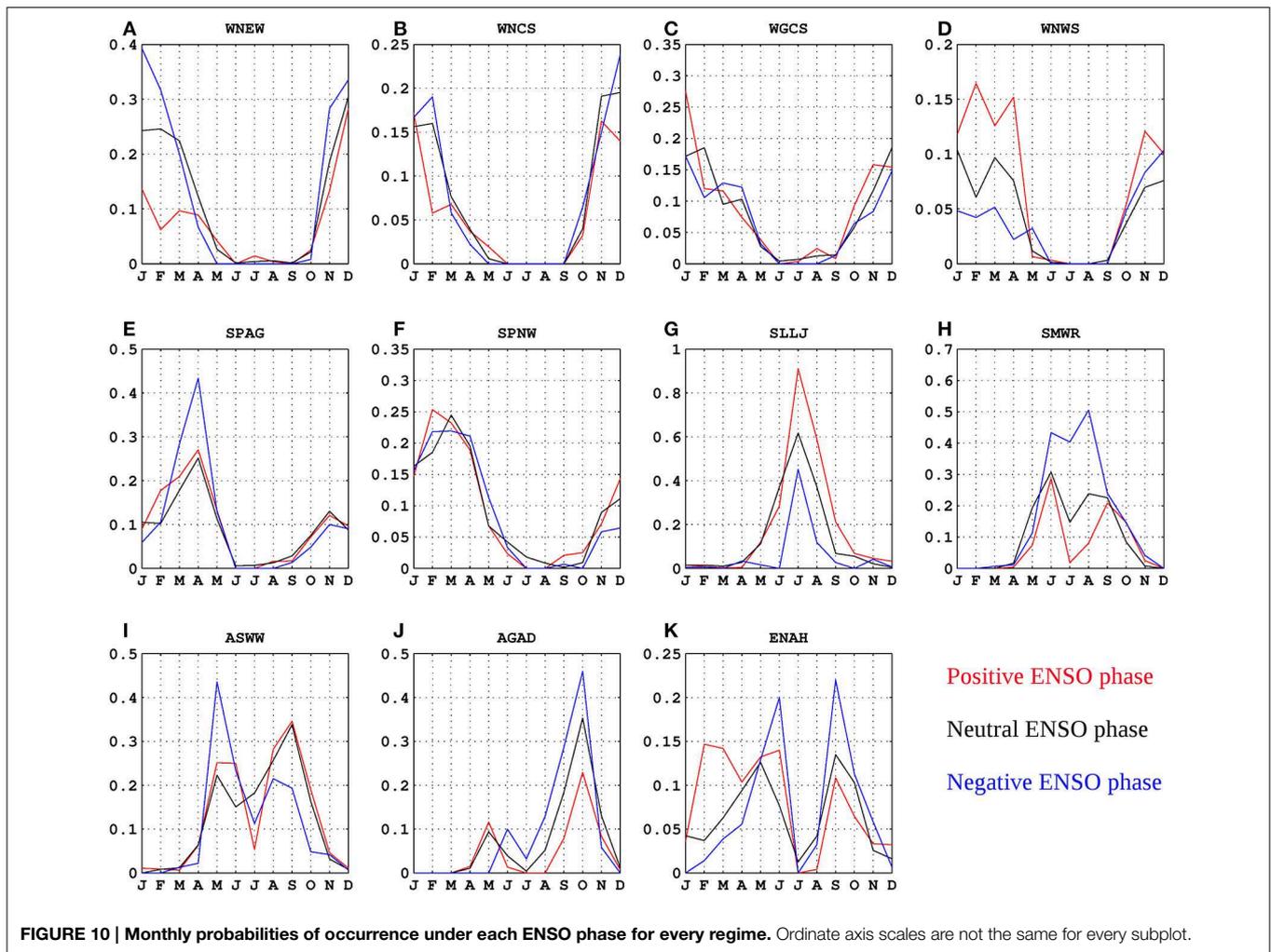
previous works by Schultz et al. (1998) and Henry (1979). The Winter North Western Surge (WNWS) was found to reproduce the structure of cold surges from the East Pacific that reach Central America, the Winter Northern Cold Surge (WNCS) was found to reproduce the structure of cold surges reaching Central America from continental North America and the Winter Gulf Cold Surge (WGCS) was linked to surges that do not reach southward of the Gulf of Mexico. Therefore, the WNWS regime is herein used as an example to study the features, evolution and effect on precipitation of CACS entering Central America. The most prominent characteristics of the WNWS regime can be summarized as: (a) west limit NASH east of the Hispaniola island, (b) trough off the United States east coast, (c) geopotential maximum east of the Sierra Madre, (d) weak trade winds and (e) enhanced gap winds at the Yucatan Peninsula and northerlies. The analysis of the WNWS events revealed that, on average, a 3 days persistence pattern of this type is preceded by WGCS like large scale conditions and that after the third day of WNWS; the following conditions do not have a determined structure. Low level winds and geopotential height depicted in **Figure 12** show the sequence associated with the development of the WNWS

pattern (11.a WGCS; 11.b, c, and d WNWS 3 day evolution). During the transition from WGCS to WNWS conditions, the low level flow through the Yucatan Peninsula is intensified. This intensification is supported by the development of a low level anticyclone in the tropical Atlantic and a cyclone in the North Atlantic. The 500 hPa fields (**Figure 13**) show how this transition is accompanied by eastward displacement of a ridge. This suggests that the west coast of North America, initially experiencing cold air advection, starts to receive warmer air. It can be also noticed how this pattern seems to be strongly linked with the subtropical jet stream. Therefore, it may be expected that this regime would be sensitive to variations in the Pacific North American region and ENSO. As the WNWS develops (**Figures 12B,C**), the intensity of the cyclone in the North eastern Pacific decreases and the winds through the topographic gaps are more intense. The flow north of the Yucatan Peninsula moves from the Tehuantepec to the Papagayo gap. The funneling due to local topography, sustains the intense westward flow over Tehuantepec. In this process, the cold surge interacts with local topography as highlighted by Steenburgh et al. (1998). The intensification of the winds west off Papagayo results from the

FIGURE 11 | Precipitation difference between warm and cold ENSO phases for (A) WNWS and (B) SLLJ regimes. Composites for cold ENSO were subtracted from composites for warm ENSO.
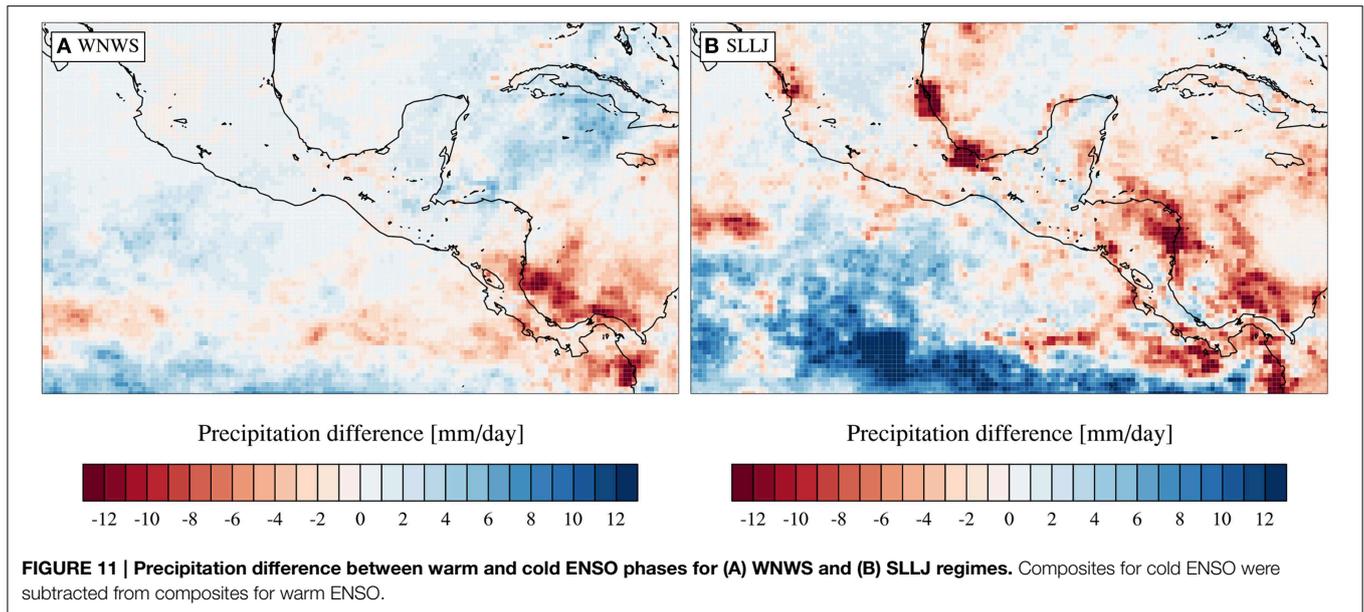
northerly flow, in agreement with the difference in the mechanisms that generate the Tehuantepec and Papagayo jets (see e.g., Chelton et al., 2000 and Romero-Centeno et al., 2007). In the upper levels (**Figure 13**), the ridges and troughs progress to the east, increasing the warm air advection until the cold air is reduced by far and the cold surge declines (**Figure 13D**).

When the northerly trades are more intense and the cold surge is developing, the circulation patterns enhance the inland transport of moisture to Central America. This moisture transport has been related to increased winter precipitation in some locations of Central America (Romero-Centeno et al., 2007). During the winter months, southernmost west coast of Central America is featured by the low level convergence.

During the stage previous to the development of the WNWS, most of the precipitation is constrained between the Yucatan and Florida Peninsulas (**Figure 14A**), alike the precipitation pattern for WGCS. As the WNWS regime develops, ITCZ precipitation increases and the nuclei of precipitation moves to the east and increases its magnitude. Precipitation is fully developed in the Caribbean coast of southern Central America and Honduras (**Figure 14B**) following the WNWS precipitation average distribution. As the system propagates to the East, the precipitating system is displaced from the Gulf of Mexico to Cuba. The eastward propagation continues as the WNWS regime reaches a mature state (**Figure 14C**). In this, precipitation has reached the Greater Antilles and is maximum over southern Central America. As the WNWS dissipates, the remaining precipitating systems leave rain in the southernmost portion of Central America (**Figure 14D**).

Discussion

The application of a weather typing approach to the classification of large scale patterns that affect Central America yielded to 11 main circulation patterns. The classification obtained is dominated by the fingerprints of wintertime circulation. This result claims winter to provide a larger variety of weather phenomena. Indeed, weather during the other seasons, particularly summer, are featured by more constrained large scale conditions. The method allowed to separate identification of the three Cold Surge patterns that are climatologically typical of the region. Namely, surges entering mostly through the Gulf of Mexico, coming from the Pacific that do not reach Central America and that can go further to Central America. Spring conditions are defined, mostly, by the position of the NASH. The eastward dislocation of the NASH induces an anticyclonic circulation over the Gulf of Mexico. Meanwhile, a more developed NASH penetrating into the Gulf is responsible for enhancement of the Trades and the development of stormy weather. Summer circulation is constrained by two of the most important features of the region, which are not necessarily independent, the monsoon regime in North America and the CLLJ.

An important link between the identified circulation types and regional precipitation was found. As the regional distribution of precipitation is characterized by a Pacific-Caribbean seesaw, each slope responds differently to the occurrence of the weather regimes. Most of winter regimes depict particular conditions of cold surges in the region. Those regimes were found to be associated with more precipitation in the Caribbean side of the isthmus. The difference among the regimes, is their ability to modify the meridional distribution of rainfall depending on their location. The drying of Central America during spring was found in consistency with reductions of precipitation under SPAG and SPNW regimes. The persistence of the ENAH regime during spring was determined to be able to trigger the onset of the rainy season in the Pacific region. Note that this regime features an eastward dislocated NASH, reducing its stabilizing impact on convective activity and low-level winds reaching the Pacific coast of Central America, thus, allowing the transport
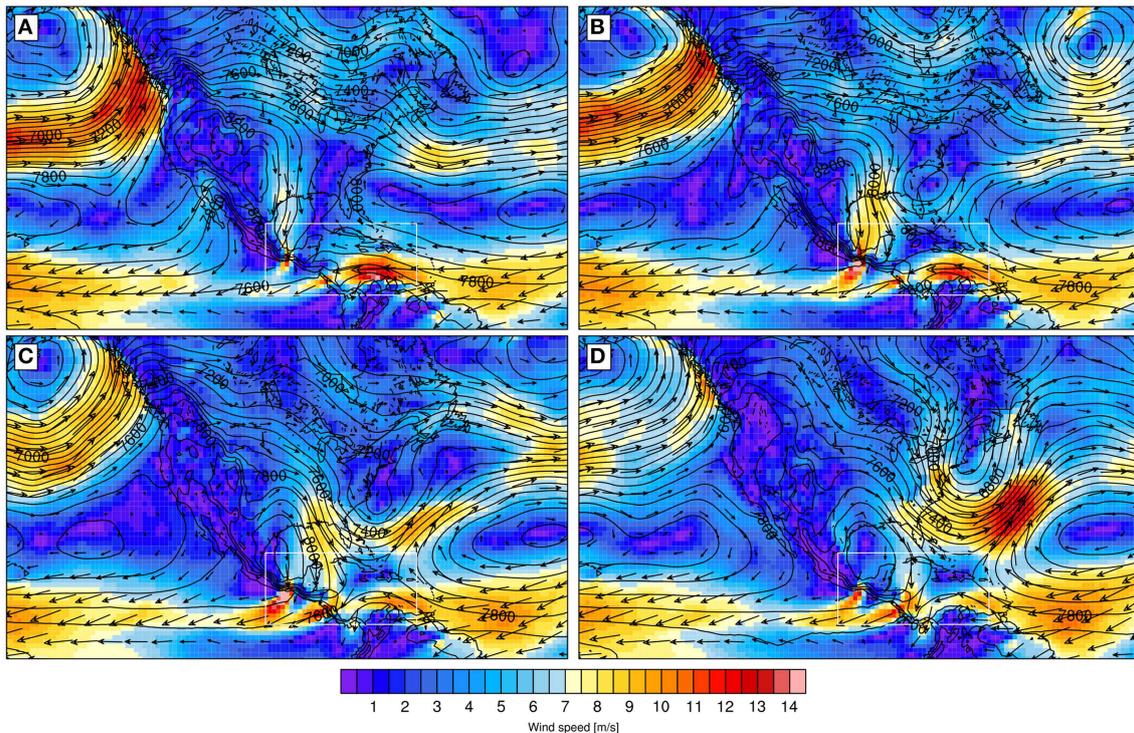
FIGURE 12 | Time evolution of a canonical WNWS event lasting 3 days. Composites for the large-scale patterns at 925 hPa for geopotential height [m/s] (black contours), wind speed [m/s] (colored pixels) and wind vectors are shown. **(A)** shows fields typical for the day previous to the onset. **(B–D)** show fields typical of days 1, 2 and 3 respectively.

of moisture from the Pacific side of the WHWP and reducing static stability.

Summer regimes were found to be consistent with the intensification of regional precipitation. Herrera et al. (2014) highlighted the importance of the CLLJ as a teleconnection mechanism between the Caribbean and the ETPac. Their analysis showed that the CLLJ is related, but not totally attached, to the NASH and other unknown mechanisms regulate its occurrence and intensity. SLLJ reflects the CLLJ peak of intensity; under this condition, convective activity at the CLLJ exit produces descending motion and dry conditions over the Pacific slope of Central America and its adjacent ocean due to adiabatic warming. Meanwhile during autumn regimes, especially AGAD, precipitation over the southwestern Caribbean increases. During this season tropical disturbances are frequent in the above mentioned Caribbean region and are likely to develop as tropical cyclones, relying on how the SST distribution and reduced vertical wind shear enhance organized deep tropical convection. Note that due to data filtering applied and the pattern-producing algorithm these tropical disturbances do not feature as particular regimes.

The ENSO mode was found to affect the frequency of occurrence of the regimes. WNEW and WNCS regimes become more frequent during cold ENSO while WGCS and WNWS are less frequent under the same ENSO phase. Under El Niño, the stronger wind flow over the Gulf of Mexico provides a more suitable environment for conditions featuring WNWS circulation to develop.

Therefore, cold air intrusions are expected to increase for warm ENSO. As shown, precipitation associated with WNWS pattern decreases for warm ENSO. According to Pérez et al. (2014) CACS occurring during warm ENSO, are related to midlatitude wave activity with shorter than typical wave lengths. This might limit the amount of time scale for orographically forced precipitation to build up and the amount of moisture the CACS can acquire from the underlying tropical ocean.

SPAG regime was determined to be more frequent during warm ENSO; however no significant precipitation changes related with this variation were detected. In contrast, the SLLJ becomes much more frequent, dominating strongly the summer circulation. Such enhancement of the CLLJ known for El Niño is fundamental to explain the interannual variability signal of drying in the Central American Pacific slope. On the Caribbean, for the same events, precipitation is intensified, suggesting a deepening of the MSD for warm ENSO.

The regime linked with the monsoonal circulation shows a strong ENSO response as the difference on its frequency for the warm and cold phases of ENSO is 2 to 1. La Niña events provide conditions to increase the veering of the Trades and favor the monsoonal moisture flow to the northern regions. Therefore, rainfall becomes more intense as enhanced low-level moisture converge reduces stability in an ambient which is already conductive for convection due to the absence of a large scale stabilizing mechanism.
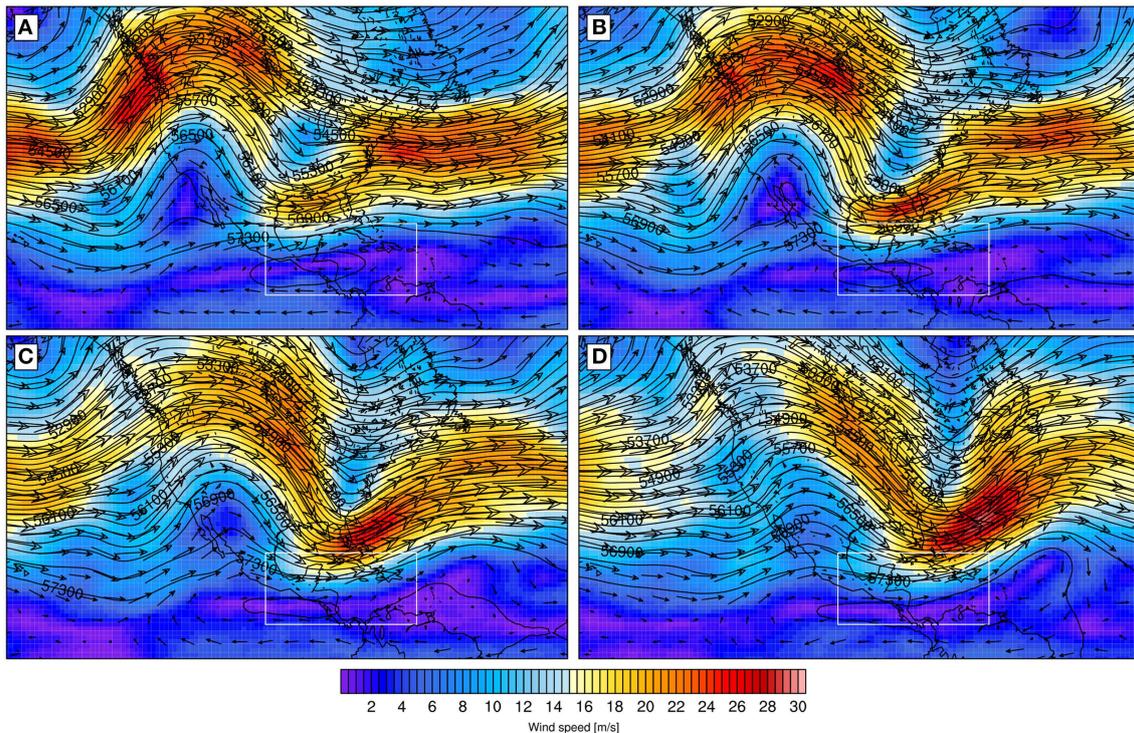
FIGURE 13 | Same as Figure 12 for 500 hPa fields. (A) shows fields typical for the day previous to the onset. **(B–D)** show fields typical of days 1, 2 and 3 respectively.

With the application of the weather types approach, the diagnostics of CACS from large scale patterns was also possible. A comparison of overlapping events detected with a previous climatological study and the present work, showed an agreement of 78%. The WNWS regime was used to study the features, evolution and effect on precipitation of CACS entering Central America. The main features of the pattern that characterizes this evolution can be listed as: (A) west limit NASH east of the Hispaniola island, (B) trough off the United States east coast, (C) geopotential maximum east of the Sierra Madre, (D) weak trade winds and (E) enhanced gap winds at the Yucatan Peninsula and northerlies.

It was determined that the development of CACS reaching Central America is composed of a transition between WGCS and WNWS conditions. For such CACS to fully develop, a 3 day persistent WNWS following WGCS was found on average.

Conclusions

This work presents the application of a weather typing approach to determine the main large scale regimes within the IAS region using publicly available data. The k-means clustering algorithm was applied to find recurrent regimes of low-level winds in this region. The number of clusters for data partitioning was selected using a criterion that measures dependency on initialization and reproducibility of the partition and 11 regimes were selected. There are recurrent low-level circulation regimes in the ERA-Interim data for the study region. Most of the regimes found were consistent with known features of the regional climate (CLLJ,

MSD, and CACS), their spatial and temporal distribution as well as their relationship with ENSO. Some of these regimes are result of regional forcing while others respond to tropical-extratropical interactions. Winter regimes are more sensitive to mid latitude forcing while summer regimes are mostly locally forced. The influence of ENSO on the regimes comes both from the tropical and extratropical response to ENSO. Winter regimes related to CACS are modulated by the effect that ENSO has on the Jet Stream, while summer regimes respond to ENSO effects on WHWP and CLLJ.

A strong link between the identified regimes and precipitation was found. Winter regimes tend to dry the Central American Pacific slope and increase precipitation on the coastal area of the Caribbean slope. Summer precipitation is highly dependent on the dominant regime; SMWR (SLLJ) favors wetter (drier) conditions to the Pacific slope while the opposite effect was found for the Caribbean. Regimes related to easterlies or North easterlies reaching Central America, produce wetter (drier) conditions on the Caribbean (Pacific). Meanwhile, regimes related with westerlies or south westerlies have the opposite effect on precipitation. Friction-induced convergence and topographic interactions are the dynamical mechanisms behind this behavior.

Three of the found regimes reflect the effect CACS have on the low-level circulation over the IAS and therefore, on precipitation. A comparison with a previous CACS climatology (Reding, 1992) was made and despite the differences found, there is a good agreement in the number of events identified as well as their duration. The identification performed in this work detected less

FIGURE 14 | Composited TRMM 3B42 precipitation estimates [mm/day] for the time evolution of a canonical 3-days WNWS event. (A) shows fields typical for the day previous to the onset. **(B–D)** show fields typical of days 1, 2 and 3 respectively.
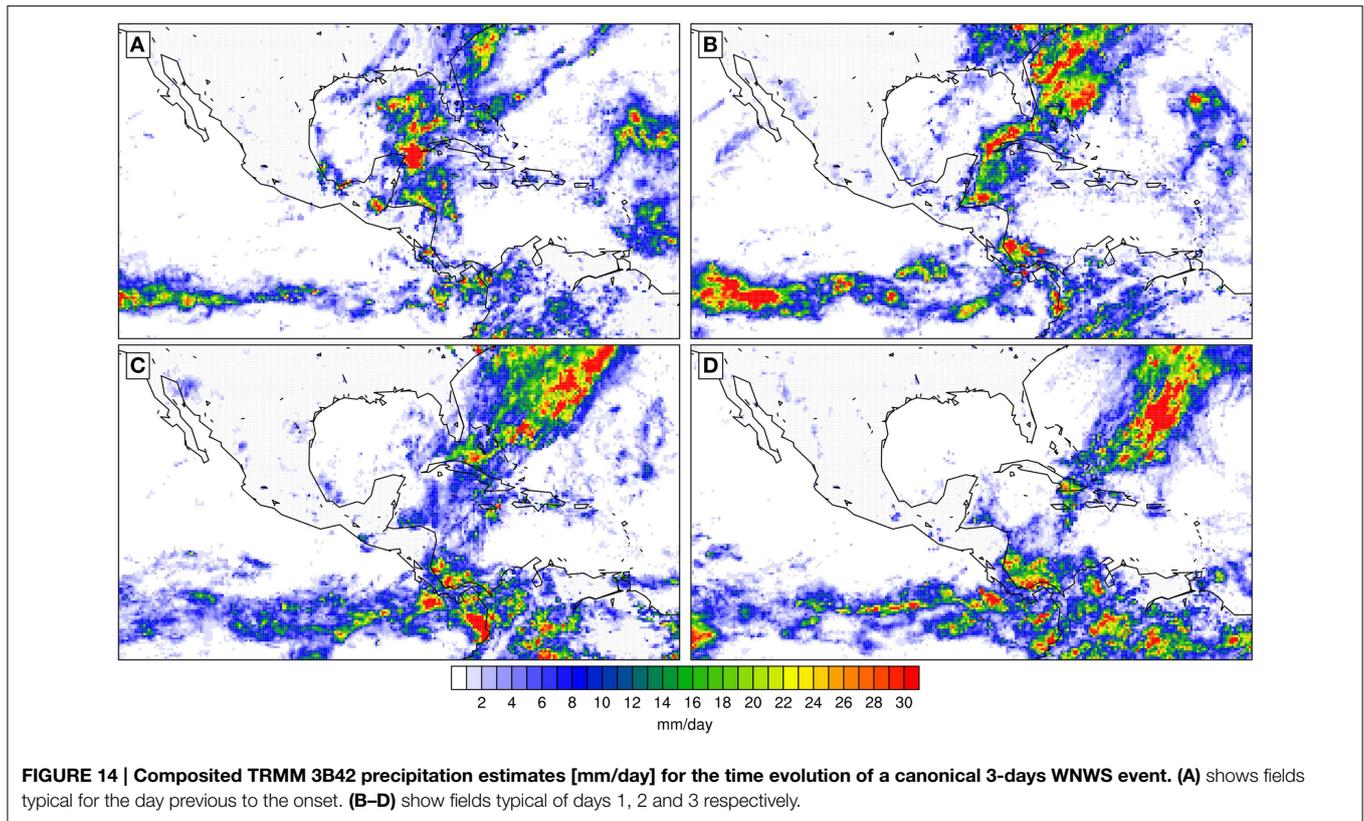
days with CACS, these differences could be due to disparities in the data nature, spatial-temporal resolution and spatial-temporal research domain. For instance, it is known that the temperature drop precedes the arrival of the anticyclonic winds in CACS. Hence, a detection method based on sub daily station data could make an earlier detection of CACS, nevertheless, an automated based on reanalysis (model) data can be used for dynamical studies and forecasting support.

The use of a weather types approach for studying circulation in the analysis domain was determined to be reliable. However, this method is largely dependent on the availability of daily data for the region and moreover, on the availability of in situ observations for validation. With the advent of new daily regional datasets in the future, we expect the application of such methods to be extremely valuable to support forecasting. Further, work is proposed to study in more detail the relationships between the large scale patterns, local forcing such as orography and observed precipitation from the point of view

of the interannual variability features mentioned in the introduction. The next step of this research would be to tag the large scale features of the tropics-extra tropics interaction via CACS development, the development of forecasting tools based on the circulation types and a proper study on the response of regional precipitation to the effect ENSO has on the large scale patterns found.

Acknowledgments

References

Alfaro, E. J. (2000). Some characteristics of the annual precipitation cycle in central america and their relationships with its surrounding tropical oceans. *Tópicos Meteorológicos y Oceanográficos* 9, 88–103.

Amador, J. (1998). A climatic feature of the tropical Americas: the trade wind easterly jet. *Tópicos Meteorológicos y Oceanográficos* 5, 91–102.

Amador, J. (2008). The intra-americas seas low-level jet (IALLJ): overview and future research. *Ann. N.Y. Acad. Sci*. 1146, 153–188. doi: 10.1196/annals.1446.012

Amador, J., Alfaro, E., Rivera, E., and Calderon, B. (2010). "Climatic features and their relationshipwith tropical cyclones over the intra-Americas Seas," in *Hurricanes and Climate Change,* Vol. 2, eds J. B. Elsner, R. E. Hodges, J. C. Malmstadt, and K. N. Scheitlin (Dordrecht: Springer Science+Bussiness Media B.V.), 149–173.

Bell, G. D., and Chelliah, M. (2006). Leading tropical modes associated with inter-annual and multidecadal fluctuations in North Atlantic hurricane activity. *J. Climate*. 19, 590–612. doi: 10.1175/JCLI3659.1

Brenes, C. L., Coen, J. D., Chelton, D. B., Enfield, D. B., Léon, S., and Ballestero, D. (2003). Wind driven upwelling in the Gulf of Nicoya, Costa Rica. *Int. J. Remote Sens*. 24, 1127–1133. doi: 10.1080/0143116021000028632

Cane, M. A., Zebiak, S. E., and Dolan, S. C. (1986). Experimental forecasts of El Nino. *Nature* 321, 827–832. doi: 10.1038/321827a0

Casola, J. H., and Wallace, J. M. (2007). Identifying weather regimes in the winter-time 500-hPa geopotential height field for the Pacific-North American sector using a limited-contour clustering technique. *J. Appl. Meteor. Climatol*. 46, 1619–1630. doi: 10.1175/JAM2564.1

Chelton, D. B., Freilich, M. H., and Esbensen, S. K. (2000). Satellite observations of the wind jets off the Pacific coast of Central America. Part I: case studies and statistical characteristics. *Mon. Wea. Rev*. 128, 1993–2018. doi: 10.1175/1520-0493(2000)128%3C1993:SOOTWJ%3E2.0.CO;2

Cheng, X., and Wallace, J. M. (1993). Cluster analysis of the northern hemisphere wintertime 500-hPa height field: spatial patterns. *J. Atmos. Sci*. 50, 2674–2696. doi: 10.1175/1520-0469(1993)050<2674:CAOTNH>2.0.CO;2

Cook, K. H., and Vizy, E. K. (2010). Hydrodynamics of the Caribbean low-level jet and its relationship to precipitation. *J. Climate* 23, 1477–1494. doi: 10.1175/2009JCLI3210.1

Cortesi, N., Trigo, R. M., Gonzalez-Hidalgo, J. C., and Ramos, A. M. (2013). Modelling monthly precipitation with circulation weather types for a dense network of stations over Iberia. *Hydrol. Earth Sys. Sci*. 17, 665–678. doi: 10.5194/hess-17-665-2013

Cortez, M. (2000). Variaciones intraestacionales de la actividad convectiva en México y América Central. *Atmósfera* 13, 95–108.

Dai, A., and Wigley, T. M. L. (2000). Global patterns of ENSO induced precipitation. *Geophys Res Lett*. 27, 1283–1286. doi: 10.1029/1999GL011140

Dee, D. P., Uppala, S. M., Simmons, A. J., Berrisford, P., Poli, P., Kobayashi, S., et al. (2011). The ERA-Interim reanalysis: configuration and performance of the data assimilation system. *Q. J. R. Meteorol. Soc*. 137, 553–597. doi: 10.1002/qj.828

Durán-Quesada, A. M., Gimeno, L., Amador, J. A., and, Nieto, R. (2010). Moisture sources for Central America: identification of moisture sources using a Lagrangian analysis technique. *J. Geophys. Res*., 115, D05103. doi: 10.1029/2009JD012455

Gamble, D. W., and Curtis, S. (2008). Caribbean precipitation: review, model and prospect. *Prog. Phys. Geogr*. 32, 265–276. doi: 10.1177/0309133308096027

Garreaud, R. D. (2001). Subtropical cold surges: regional aspects and global distribution. *Int. J. Climatol*. 21, 1181–1197. doi: 10.1002/joc.687

Giannini, A., Saravanan, R., and Chang, P. (2003). Oceanic forcing of sahel rainfall on interannual to interdecadal time scales. *Science* 302, 1027–1030. doi: 10.1126/science.1089357

Goldenberg, S. B., and Shapiro, L. J. (1996). Physical mechanisms for the association of El Nino and West African rainfall with Atlantic major hurricane activity. *J. Clim*. 9, 1169–1187.

González, C. (1999). Climatología de los frentes fríos que han afectado a Cuba desde 1916-1917 hasta 1996-1997. *Rev. Cubana de Meteorol*. 6, 15–19.

Henry, W. K. (1979). Some aspects of the fate of cold fronts in the Gulf of Mexico. *Mon. Wea. Rev*. 107, 1078–1082. doi: 10.1175/1520-0493(1979)107<1078:SAOTFO>2.0.CO;2

Herrera, E., Magaña, V., and Caetano, E. (2014). Air–sea interactions and dynamical processes associated with the midsummer drought. *Int. J. Climatol*. doi: 10.1002/joc.4077

Huffman, G. J., Adler, R. F., Bolvin, D. T., and Nelkin, E. J. (2010). "The TRMM Multi-satellite Precipitation Analysis (TMPA)," in *Satellite Rainfall Applications for Surface Hydrology,* eds F. Hossain and M. Gebremichael (Dordrecht: Springer Science+Bussiness Media B.V), 3–22.

Karnauskas, K. B., Giannini, A., Seager, R., and Busalacchi, A. J. (2013). A simple mechanism for the climatological midsummer drought along the Pacific coast of Central America. *Atmósfera* 26, 261–281. doi: 10.1016/S0187-6236(13)71075-0

Kerr, R. A. (2000). A north atlantic climate pacemaker for the centuries. *Science* 288, 1984–1986. doi: 10.1126/science.288.5473.1984

Knight, J. R., Folland, C. K., and Scaife, A. A. (2006). Climate impacts of the Atlantic multidecadal oscillation. *Geophysi. Res. Lett*. 33:L17706. doi: 10.1029/2006GL026242

Lamb, H. H. (1950). Types and spells of weather around the year in the British Isles: annual trends, seasonal structure of the year, singularities. *Q. J. R. Meteorol. Soc*. 76, 393–429. doi: 10.1002/qj.49707633005

MacQueen, J. (1967). "Some methods for classification and analysis of multivariate observations," in *Fifth Berkeley Symposium on Mathematics, Statistics and Probability* (University of California Press). 281–297.

Magaña, V., Amador, J., and Medina, S. (1999). The Midsummer Drought over Mexico and Central America. *J. Climate*. 12, 1577–1588. doi: 10.1175/1520-0442(1999)0122.0.CO;2

Magaña, V., and Vázquez, J. (2000). "Interannual variability of Northern activity over the Americas," in *Reprints of the 24th Conference on Hurricanes and Tropical Meteorology*. (Ft. Lauderdale, FL), 116–111.

Malmgren, B. A., Winter, A., and Chen, D. (1998). El Niño-southern oscillation and North Atlantic oscillation control of climate in Puerto Rico. *J. Clim*. 11, 2713–2717.

Mantua, N. J., Hare, S. R., Zhang, Y., Wallace, J. M., and Francis, R. C. (1997). A Pacific interdecadal climate oscillation with impacts on salmon production. *Bull. Amer. Meteor. Soc*. 78, 1069–1079.

Méndez, M., and Magaña, V. (2010). Regional aspects of prolonged meteorological droughts over Mexico and Central America. *J. Clim*. 23, 1175–1188. doi: 10.1175/2009JCLI3080.1

Michelangeli, P. A., Vautard, R., and Legras, B. (1995). Weather regimes: recurrence and quasi stationarity. *J. Atmos. Sci*. 52, 1237–1256. doi: 10.1175/1520-0469(1995)052<1237:WRRAQS>2.0.CO;2

Molteni, F., Kucharski, F., and Corti, S. (2006). "On the predictability of flow-regime properties on interannual to interdecadal timescales," in *Predictability of Weather and Climate*, eds T. Palmer and R. Hagedorn (Cambridge: Cambridge University Press), 365–390.

Moron, V., Robertson, A. W., and Qian, J.-H. (2010). Local versus regional-scale characteristics of monsoon onset and post-onset rainfall over Indonesia. *Clim Dyn*. 34, 281–299. doi: 10.1007/s00382-009-0547-2

Moron, V., Robertson, A. W., Ward, N., and Ndiaye, O. (2008). Weather types and rainfall over senegal. Part I: observational Analysis. *J. Clim*. 21, 266–287. doi: 10.1175/2007JCLI1601.1

Muñoz, E., Busalacchi, A. J., Nigam, S., and Ruiz-Barradas, A. (2008). Winter and summer structure of the Caribbean low-level jet. *J. Clim*. 21, 1260–1276. doi: 10.1175/2007JCLI1855.1

Perez, E., Magaña,V., Caetano E., and Kusunoki, S. (2014). Cold surge activity over the Gulf of Mexico in a warmer climate. *Front. Earth Sci*. 2:19. doi: 10.3389/feart.2014.00019

Pezzi, L. P., and Cavalcanti, I. F. A. (2001). The relative importance of ENSO and tropical Atlantic sea surface temperature anomalies for seasonal precipitation over South America: a numerical study. *Clim. Dyn*. 17, 205–212. doi: 10.1007/s003820000104

Qian, J.-H., Robertson, A. W., and Moron, V. (2010). Interactions among ENSO, the Monsoon, and Diurnal Cycle in Rainfall Variability over Java, Indonesia. *J. Atmos. Sci*. 67, 3509–3524. doi: 10.1175/2010JAS 3348.1

Reding, P. J. (1992). *The Central American Cold Surge: an Observational Analysis of the Deep Southward Penetration of North America Cold Fronts*. MSc. thesis, Department of Meteorology, Texas A&M University, Rogers.

Rogers, J. C. (1984). The association between the North Atlantic oscillation and the Southern oscillation in the Northern Hemisphere. *Mon. Wea. Rev*. 112. 1999–2015.

Romero-Centeno, R., Zavala-Hidalgo, J., and Raga, G. B. (2007). Midsummer gap winds and low-level circulation over the eastern tropical Pacific. *J. Clim*. 20, 3768–3784. doi: 10.1175/JCLI4220.1

Ropelewski, C. F., and Halpert, M. S. (1987). Global and regional scale precipitation patterns associated with the El Nino/ Southern Oscillation. *Mon. Wea. Rev*. 115, 1606–1626.

Schultz, D. M., Bracken, W. E., and Bosart, L. F. (1998). Planetary- and synoptic-scale signatures associated with Central American Cold Surges. *Mon. Wea. Rev*. 126, 5–27. doi: 10.1175/1520-0493(1998)126<0005:PASSSA>2.0.CO;2

Schultz, D. M., Bracken, W. E., Bosart, L. F., Hakim, G. J., Bedrick, M. A., Dickinson, M. J., et al. (1997). The 1993 superstorm cold surge: frontal structure, gap flow, and tropical impact. *Mon. Wea. Rev*. 12, 5–39. doi: 10.1175/1520-0493(1997)125<0005:TSCSFS>2.0.CO;2

Simpson, J., Adler, R. F., and North, G. R. (1988). A proposed tropical rainfall measuring mission (TRMM) satellite. *Bull. Amer. Meteor. Soc.* 69, 278–295.

Small, R. J. O., De Szoeke, S. P., and Xie, S. P. (2007). The Central American Midsummer Drought: regional aspects and large-scale forcing*. *J. Clim.* 20, 4853–4873. doi: 10.1175/JCLI4261.1

Steenburgh, W. J., Schultz, D. M., and Colle, B. A. (1998). The structure and evolution of gap outflow over the Gulf of Tehuantepec, Mexico. *Mon. Wea. Rev.* 126, 2673–2691.

Straus, D. M., and Molteni, F. (2004). Circulation regimes and SST forcing: results from large GCM ensembles. *J. Clim.* 17, 1641–1656. doi: 10.1175/1520-0442 (2004)017<1641:CRASFR>2.0.CO;2

Trigo, R. M., and DaCamara, C. C. (2000). Circulation weather types and their influence on the precipitation regime in Portugal. *Int. J. Climatol.* 20, 1559–1581. doi: 10.1002/1097-0088(20001115)20:13%3C1559::AID-JOC555%3E3.0.CO;2-5

Turner, A. G., Inness, P. M., and Slingo, J. M. (2005). The role of the basic state in the ENSO–monsoon relationship and implications for predictability. *Q. J. R.* 131, 781–804. doi: 10.1256/qj.04.70

Wang, C. (2007). Variability of the Caribbean low-level jet and its relations to climate. *Clim Dyn.* 29, 411–422. doi: 10.1007/s00382-007-0243-z

Wang, C., and Enfield, D. B. (2001). The tropical Western Hemisphere warm pool. *Geophys. Res. Lett.* 28, 1635–1638. doi: 10.1029/2000GL011763

Wang, C., and Enfield, D. B. (2003). A further study of the tropical Western Hemisphere warm pool. *J. Clim.* 16, 1476–1493. doi: 10.1175/1520-0442-16.10.1476

Wang, C., and Lee, S.-K. (2007). Atlantic warm pool, Caribbean low-level jet, and their potential impact on Atlantic hurricanes. *Geophys. Res. Lett.* 34, L02703. doi: 10.1029/2006GL028579

Wang, C., Lee, S. K., and Enfield, D. B. (2007). Impact of the Atlantic warm pool on the summer climate of the Western Hemisphere. *J. Clim.* 20, 5021–5040. doi: 10.1175/JCLI4304.1

Wolter, K., and Timlin, M. S. (2011). El Niño/Southern Oscillation behaviour since 1871 as diagnosed in an extended multivariate ENSO index (MEI. ext). *Inter. J. Climatol.* 31, 1074–1087. doi: 10.1002/joc.2336

Yu, B., and Wallace, J. M. (2000). The principal mode of interannual variability of the North American monsoon system. *J. Clim.* 13, 2794–2800. doi: 10.1175/1520-0442(2000)013%3C2794:TPMOIV%3E2.0.CO;2

Zárate, E. (2013). Climatología de masas invernales de aire frío que alcanzan Centroamérica y el Caribe y su relación con algunos índices Árticos. *Tópicos Meteorológicos y Oceanográficos* 12, 35–55.

Zhang, R., and Delworth, T. L. (2006). Impact of Atlantic multidecadal oscillations on India/Sahel rainfall and Atlantic hurricanes. *Geophys. Res. Lett.* 33:L17712. doi: 10.1029/2006GL026267